Economic Geology
Vol. 83, 1988, pp. 551–567

Relationships between a Porphyry Cu-Mo Deposit, Base and Precious Metal Veins, and Laramide Intrusions, Mineral Park, Arizona

JAMES R. LANG AND CHRISTOPHER J. EASTOE

Department of Geosciences, University of Arizona, Tucson, Arizona 85721

Abstract

In the Wallapai mining district, porphyry-style copper-molybdenum mineralization occurs within and near Laramide granitoid stocks at the center of an elongate zone of polymetallic quartz veins. The principal mineralized veins form a well-defined paragenetic sequence, with a simplified mineralogy progressing through: (1) anhydrite-molybdenite (AM) veins of quartz + K-feldspar + anhydrite + pyrite + biotite + molybdenite, (2) quartz-molybdenite (QM) veins with quartz + molybdenite + pyrite, (3) anhydrite-chalcopyrite (AC) veins containing quartz + K-feldspar + anhydrite + pyrite + magnetite + chalcopyrite + chlorite + rutile, (4) quartz-pyrite (QP) veins of quartz + sericite + pyrite, and quartz + pyrite + chalcopyrite + epidote + chlorite, and (5) polymetallic quartz (PMQ) veins, with a gangue assemblage of quartz + sericite + calcite + kaolinite(?) + epidote + chlorite, and a variety of base and precious metal minerals.

The coexistence of vapor- and liquid-rich fluid inclusions in vein quartz shows that the molybdenite-bearing anhydrite and quartz veins formed at 360° to 410°C from boiling, low-salinity brines. Chalcopyrite deposition in the anhydrite-chalcopyrite veins was at 380° to 420°C from nonboiling brines averaging 20 equiv wt percent NaCl and 25 equiv wt percent KCl. The quartz-pyrite veins formed at 320° to 350°C from brines of 1 to 13 equiv wt percent NaCl. The polymetallic quartz veins formed from dilute brines of 1 to 7 equiv wt percent NaCl. Temperatures in the first stage of mineralization of the polymetallic-quartz veins abruptly increased to 400° to 450°C in and near Mineral Park, but declined outward to less than 300°C on the district periphery. In subsequent stages, fluid temperatures decreased across the district to less than 200°C. Pressures were 250 to 300 bars, probably in a hydrostatic pressure regime, during boiling related to molybdenite mineralization, but they may have increased to about 1,100 bars lithostatic pressure during chalcopyrite deposition in the anhydrite-chalcopyrite veins. A depth during mineralization of 3 to 4 km is suggested.

Copper and molybdenum mineralization occurred in a lithocap environment above a progenitor intrusion but was not directly related to the exposed Ithaca Peak stocks. The evolution from hypersaline fluids in the anhydrite-chalcopyrite veins to low-salinity, lower temperature fluids in the quartz-pyrite veins suggests an influx of meteoric water into the waning porphyry-style hydrothermal system. Brines up to 100°C hotter appeared during the formation of the paragenetically later polymetallic quartz veins and constituted a new, and much larger, hydrothermal system. The heat source, presumably an unexposed intrusion, was much larger than the porphyry-style system. The zonation in base metal ratios of polymetallic quartz veins is symmetrical with respect to the proposed heat source.

Introduction

SEVERAL porphyry-style deposits have peripheral, zoned base and precious metal mineralization, e.g., Bingham Canyon, Utah (John, 1978), the Pima district, Arizona (Titley, 1982b), Butte, Montana (Meyer et al., 1968), and the Wallapai district, Arizona (Eidel et al., 1968; Wilkinson et al., 1982). Such mineralization may occur as large polymetallic quartz-sulfide veins, carbonate replacement ores, or lead-zinc skarn deposits. The peripheral ores have contributed significantly to the production of most of these porphyry-cored districts. Lead, zinc, copper, silver, and gold are typically the major commodities. At Butte, manganese and arsenic have also been produced (Meyer et al., 1968).

Although this spatial association of porphyry and peripheral mineralization has been frequently noted, few integrated geochemical studies have been undertaken to evaluate possible genetic relationships. The Wallapai district contains both porphyry copper-molybdenum mineralization at Mineral Park and an extensive system of numerous, well-exposed, peripheral polymetallic base and precious metal veins. It is an excellent setting in which to evaluate the thermal, isotopic, and chemical relationships of these mineralization styles. In this paper we will focus on a fluid inclusion study of the Wallapai mining district. These results form part of a broader study encompassing sulfur and oxygen isotopes and chemical considerations that is to be presented later.

0361-0128/88/804/551-17$2.50

In carrying out this study, we have combined new fluid inclusion and petrographic data with a body of existing data (Wilkinson, 1981; Wilkinson et al., 1982). Our current interpretations, therefore, depend significantly on the results of earlier workers at the University of Arizona, particularly W. H. Wilkinson and S. R. Titley.

The Wallapai mining district is located 25 km north of Kingman, Arizona, in the Cerbat Mountains (Fig. 1). The boundaries of the 130-km^2 district are defined by the extent of polymetallic quartz veins. The principal deposit in the district is the Mineral Park porphyry-style copper-molybdenum orebody, which occurs at the center. Currently closed, Mineral Park has produced approximately 323,000 short tons of copper, 25,000 short tons of molybdenum and 5,000,000 oz of silver since the initiation of open-pit operations in 1964 (Wilkinson et al., 1982). Mineral Park contains mineable reserves of 50 million short tons grading 0.20 percent Cu and 0.051 percent Mo (Wilkinson et al., 1982). The polymetallic quartz veins, which surround Mineral Park, produced gold, silver, lead, zinc, and copper from 1863 through the 1940s. The Tennessee-Schuylkill and the Golconda mines were the only significant vein producers. They yielded a total of 590 short tons of copper, 31,000 short tons of lead, 61,500 short tons of zinc, 2,024,367 oz of silver and 63,135 oz of gold (Dings, 1951).

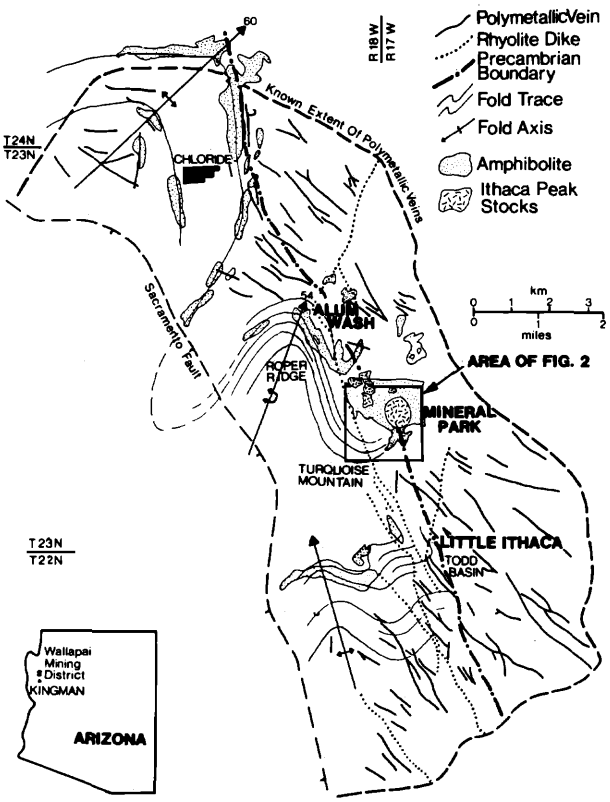

FIG. 1. Generalized geology of the Wallapai mining district, Arizona. Geologic features are simplified and have been modified from figure 26.4 of Wilkinson et al. (1982). The rectangle surrounding Mineral Park delineates the area shown in Figure 2.

General Geology

The principal methods of this study were geochemical in nature and did not involve mapping or extensive examination of lithologies in the district. The reader who requires more detailed descriptions of general geologic features should consult the studies by Thomas (1949, 1953), Dings (1951), Eidel et al. (1968), Eaton (1980), Wilkinson et al. (1982), and Vega (1984). The majority of the lithologic and structural information that follows has been summarized from the work of these authors.

Lithology

The oldest rocks in the district are a conformable sequence of folded metasedimentary and metavolcanic units including amphibolite, quartz-feldspar gneiss, biotite schist, hornblende-diopside schist, and minor quartzite (Thomas, 1949). This sequence was intruded by a biotite granite to biotite quartz monzonite batholith having a U-Pb zircon age of 1,740 ± 20 m.y. (Silver, 1967, using old decay constants). The batholith contains abundant amphibolite xenoliths near its margin and has been metamorphosed to gneiss. The Diana Granite cuts the folded sequence and has a K-Ar date of 1,340 ± 20 m.y. (Shafiqullah et al., 1980). All Precambrian rocks have been metamorphosed to the upper greenschist-lower amphibolite facies. No record of events between Proterozoic and Laramide time has been preserved.

Laramide time is represented by the Ithaca Peak stocks, porphyry copper-molybdenum mineralization and associated alteration, rhyolitic and intermediate dikes, and possibly, polymetallic quartz veins. The Ithaca Peak stocks include two bodies, one of quartz monzonite porphyry and the other of biotite-quartz diorite porphyry to biotite-quartz monzonite porphyry (Fig. 2). The stocks contain phenocrysts of quartz, biotite, plagioclase, and K-feldspar in a fine-grained groundmass of quartz, orthoclase, and biotite. Each of these intrusions is 600 to 800 m in diameter and shows slight textural and mineralogical variations. Mauger and Damon (1965) reported a K-Ar age of 73.3 ± 2.6 m.y. (modified for new decay constants) on vein biotite from Ithaca Peak, establishing a minimum age of intrusion.

Structure

Foliations and folds: Foliations in the Precambrian rocks are defined by the alignment of biotite

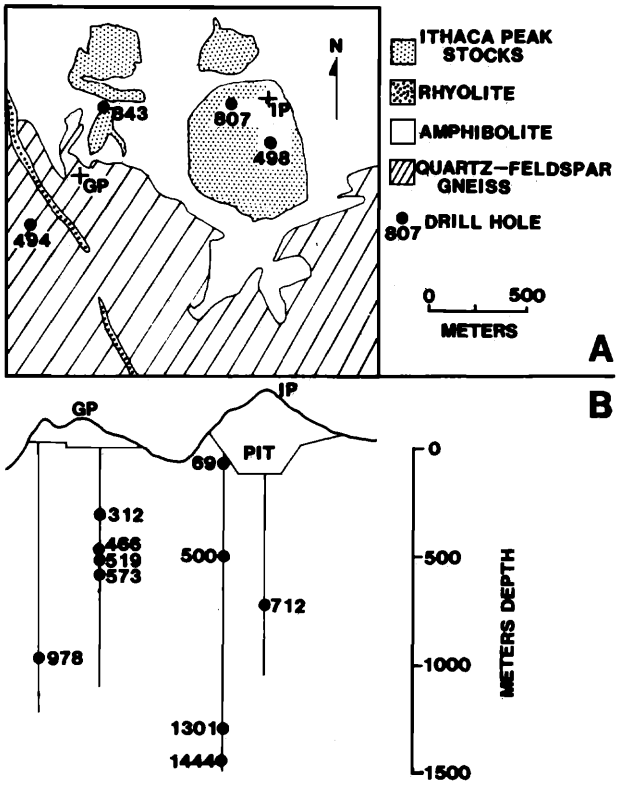

FIG. 2. Simplified geology and location of sampled drill holes at Mineral Park (A), and the vertical distribution of drill hole samples (B). Geology is after Wilkinson (1981). The depth profiles of the drill holes in B are aligned with their surface location in A. The area of this figure is outlined in Figure 1. IP = Ithaca Park; GP = Gross Peak.

grains. Foliations in the eastern part of the district have consistent trends of N 30°–50° E, whereas foliations in the western portion show variable orientations. This phenomenon led Wilkinson (1981) to subdivide the district into two structural domains. The boundary between the domains (called the Precambrian contact in subsequent references) generally coincides with the intrusive contact between the 1,740-m.y.-old batholith and the older, folded Proterozoic sequence; the boundary runs the length of the district and trends N 30° W (Fig. 1).

Foliations and amphibolite layers within the western domain are affected by several major folds (Fig. 1). The fold axes trend north to N 45° E with steep northeast plunges of 55° to 65° (Wilkinson, 1981). Eaton (1980) suggested as many as three folding episodes. Alteration, mineralization, and intrusive activity have been localized where fold axes of the western domain are truncated by the Precambrian contact (Wilkinson, 1981). The porphyry-style alteration and mineralization at Alum Wash, Mineral Park, and Little Ithaca are located where the Roper Ridge, Turquoise Mountain, and Todd Basin folds, respectively, are truncated by the Precambrian contact (Fig. 1).

Faults: Faults are numerous and widespread throughout the district and are most apparent when they are occupied by dike rocks or veins. The faults trend N 30°–60° W and dip steeply to the northeast and southwest (Eaton, 1980). They lie subparallel to the Precambrian contact and are approximately centered around it. They deviate from the general trend where they follow lithologic contacts around the nose of the Chloride antiform (Wilkinson, 1981). A lack of marker units precludes an accurate determination of offset. Slickensides observed underground in the C.O.D. mine indicate that the latest episode of movement was oblique or normal dip slip. Movement before, during, and after vein deposition has been recognized. Eaton (1980) noted that some of the faults contain metamorphosed and deformed Precambrian(?) rhyolite dikes, suggesting that many of these faults are long-established structures which may have undergone periodic reactivation.

The Sacramento fault lies mostly buried beneath alluvium in the Sacramento Valley west of the Cerbat Mountains (Thomas, 1949). It juxtaposes middle Tertiary volcanic rocks against Precambrian crystalline rocks and is most likely a basin-and-range feature whose principal effect has been a tilting of the Cerbat Mountain 15° to the east (Thomas, 1953).

Porphyry-Style Alteration and Mineralization

Alteration effects at Mineral Park are subdivided into the selectively pervasive and veinlet-controlled styles of Titley (1982a). Sample locations of this study are shown in Figure 2 and later in Figure 5. The information on paragenetic sequence and wall-rock control in Table 1 is based on the observations of Wilkinson (1981), with a few modifications. All vein stages occur within the porphyry deposit proper, but only the polymetallic quartz veins occur outside it. The vein designations in this study are new and indicate characteristic mineralogy.

Anhydrite-molybdenite (AM) veins

The mineralogy and the coexisting mineral assemblages of anhydrite-molybdenite veins vary with position in the vein. Molybdenite is invariably found at the contact of the vein with its host rock, in association with fine-grained quartz containing rare solid inclusions of biotite and anhydrite. The basic coexisting assemblage is quartz + molybdenite + biotite + anhydrite. In the center of the veins quartz is more coarse-grained and is laced with abundant solid inclusions of anhydrite, K-feldspar, pyrite, and biotite, which together with depositional textures, suggests a coexisting assemblage of

TABLE 1. Paragenetic Sequence of Major Vein Stages and Associated Host-Rock Alteration

Stage	Mineralogy	Alteration effects	
		Felsic host rocks	Mafic host rocks
Pervasive biotite	Bt ± qtz ± mt	Bt replaces igneous bt; disseminations	Rut after primary bt; bt replaces hbl and bt
Pervasive K-feldspar	Kspar	Kspar replaces primary igneous kspar	Kspar replaces plag
Early biotite veins	Bt ± (qtz, mt)	None	Bt replaces hbl
Early K-feldspar veins	Kspar ± (bt, qtz)	Diffuse contacts	None
Anhydrite-molybdenite (AM) veins	Qtz + kspar + anhy + py + bt + moly ± (cal, cpy)	Kspar selvedges; minor cal replaces plag	Bt replaces hbl and primary bt
Quartz-molybdenite (QM) veins	Qtz + moly ± py	None	Minor bt replaces hbl
Anhydrite-chalcopyrite (AC) veins	Qtz + kspar + anhy + py + mt + cpy + chl + rut ± (ep, bt, cal, ab, sl, gl)	Bt replaces primary bt; chl replaces secondary bt	Chl replaces bt and hbl; cpy occupies up to 10 percent of mafic sites
Quartz-pyrite (QP) veins	Qtz + ser + py ± cpy ± cal or Qtz + py + cpy + cal + ep + chl + (ser)	Ser replaces plag, kspar and bt in wide halos	Chl replaces bt and hbl; cal and ser after plag
Polymetallic quartz (PMQ) veins	See Figure 4	Early intense silicification followed by intense phyllic alteration adjacent to the vein; late argillic alteration with sphene	

Modified from Wilkinson et al. (1982); minerals in parentheses are trace constituents

Abbreviations: ab = albite, anhy = anhydrite, bt = biotite, cal = calcite, chl = chlorite, cpy = chalcopyrite, ep = epidote, gl = galena, hbl = hornblende, kspar = K-feldspar, moly = molybdenite, mt = magnetite, plag = plagioclase, py = pyrite, qtz = quartz, rut = rutile, ser = sericite, sl = sphalerite

quartz + K-feldspar + anhydrite + biotite + pyrite. Chalcopyrite is another trace vein constituent that is found in the central portions of these veins. It does not occur as solid inclusions in any of the other vein minerals and was not observed in contact with molybdenite, so that its relationship to molybdenite cannot be ascertained. The transition from the edge to the center of an anhydrite-molybdenite vein is characterized by a gradational inward increase in both quartz grain size and the number of solid inclusions within the quartz.

Quartz-molybdenite (QM) veins

Quartz + molybdenite ± pyrite veins crosscut anhydrite-molybdenite (Wilkinson et al., 1982). Molybdenite is most commonly found at the contact of veins and wall rock, whereas pyrite is confined to the center of the vein structure. Quartz occurs throughout these veins with no textural variation.

Anhydrite-chalcopyrite (AC) veins

The assemblage in these veins is quartz + K-feldspar + pyrite + sphalerite + biotite + anhydrite + rutile + chalcopyrite + minor magnetite + calcite + chlorite. Intergrowth textures and solid inclusion distributions suggest that quartz + K-feldspar + pyrite + sphalerite + biotite + magnetite + anhydrite + rutile are contemporaneous. Where in contact, magnetite and pyrite are intergrown. Chalcopyrite is much more abundant in anhydrite-chalcopyrite veins than in anhydrite-molybdenite veins, but its relationship to other phases is uncertain. Calcite and chlorite appear to replace all other minerals. Biotite is a previously unreported phase. Albite and galena were both noted by Wilkinson (1981) but were not observed in this study; these minerals and epidote are trace constituents and their position in the paragenetic sequence is unknown. There is no zonation from edge to center in these veins.

Quartz-pyrite (QP) veins

These veins were an important source of copper for the mining operation (Wilkinson et al., 1982). They contain up to 1 vol percent hypogene chalcopyrite, and chalcocite occurs as a supergene replacement of hypogene pyrite. The assemblage of coexisting minerals varies as a function of host-rock lithology. Within felsic host rocks the quartz-pyrite vein mineralogy is quartz + sericite + pyrite + minor calcite ± chalcopyrite. The vein mineralogy changes to quartz + pyrite + calcite + chlorite + epidote ± sericite ± chalcopyrite where they cut mafic host rocks. Quartz-pyrite veins cut anhydrite-molybdenite, quartz-molybdenite, and anhydrite-chalcopyrite veins (Wilkinson et al., 1982).

Polymetallic quartz (PMQ) veins

Physical features: Polymetallic quartz veins are planar to gently curving structures with steep northeast and southwest dips of greater than 60°

(Eaton, 1980). They generally conform to the N 30°–50° W structural grain of the district (Fig. 1). The traceable strike length of individual veins ranges from 30 m to 4 km (Thomas, 1949), with an aggregate surface trace of 140 km (Dings, 1951). Individual veins range from 10 cm to 10 m wide (Dings, 1951), and composite mineralized zones of several closely spaced veins reach 25 m in width (Thomas, 1949). The veins pinch and swell along strike and downdip with numerous but minor strike changes. Polymetallic quartz veins commonly crop out as iron-stained siliceous boxworks of prominent positive relief.

Polymetallic quartz veins characteristically consist of bands of coherent quartz-sulfide material alternating with fault gouge, in which crushed and rolled quartz sulfide and wall-rock fragments are found. Crustification banding and other open-space-filling textures are common.

Age: The age of the polymetallic quartz veins, possibly Laramide or mid-Tertiary, is uncertain. Unmetamorphosed and undeformed rhyolite dikes of probable Laramide age crosscut, and are crosscut by, the early stages of porphyry mineralization (Wilkinson, 1981; Vega, 1984). These veins have been reported (Eaton, 1980; Wilkinson et al. 1982; Vega, 1984) as being cut by these same rhyolite dikes, but the reverse has not been noted.

Petrography and paragenetic sequence: Samples were obtained from mine dumps throughout the district and from underground workings at the C.O.D. mine. The paragenetic sequence presented in Figure 3 is based on typical mineral relationships noted throughout the district, though minor differences sometimes occur between individual veins. In addition to the minerals listed, the following trace minerals have been reported: hypogene pearceite and polybasite (Bastin, 1925), and fluorite, stibnite, proustite, pyrargyrite, and miargyrite (Thomas, 1949). Vein formation is separated into four distinct stages on the basis of consistent replacement textures and brecciation events recognized in both polished thin sections and outcrop.

In stage 1, mineralization is typified by strong silicification accompanied by minor pyrite and trace arsenopyrite. Trace amounts of sericite occur. Pyrrhotite was the first sulfide to appear and was replaced by pyrite. The transition between stage 1 and stage 2 mineralization is invariably marked by a brecciation event.

The vein material in stage 2 is typically crustified. There are two substages, 2a and 2b, that differ in mineralogy. In both substages quartz is the major gangue mineral and sericite is abundant; carbonates and hypogene clay (kaolinite?) are present in minor quantities. In 2a, pyrite and arsenopyrite in large subequal volumes are the dominant sulfides; minor

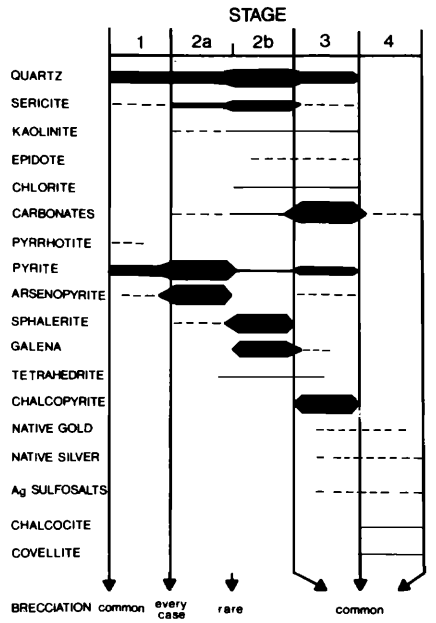

FIG. 3. Mineral paragenetic sequence of polymetallic quartz (PMQ) veins. Major mineral abundance is relative to bar widths. Minor phases are represented by thin solid lines, trace phases by dashed lines. The relative frequency of brecciation between each stage of mineralization is indicated at the bottom.

sphalerite is found in crustification bands. In 2b, the sulfide fraction is dominated by sphalerite, galena, and minor tetrahedrite; pyrite is a trace constituent and arsenopyrite is absent. The end of stage 2 deposition is usually, but not invariably, marked by a second episode of brecciation.

Carbonates and quartz occur in approximately equal amounts in stage 3. Sericite and kaolinite(?) are present, and chlorite and epidote appear as minor phases. Chalcopyrite is the principal ore mineral, veining and replacing all other hypogene minerals. Pyrite is the only other abundant sulfide. Sphalerite is absent, and galena and arsenopyrite occur as minor constituents. Native gold was observed only in the Arizona Magma mine, where it replaces pyrite and arsenopyrite from stages 1 and 2a. Native silver may have formed as a hypogene mineral in stage 3 but is very likely a supergene mineral (see below). The temporal position of the sulfosalt phases is based on sketches found in Bastin (1925) which show sulfosalts in association with chalcopyrite and veining both galena and sphalerite. Deposition of stage 3 mineralization is usually terminated by a third brecciation event.

Stage 4 consists of numerous supergene minerals, which were listed by Thomas (1949). Garrett (1938) noted that galena in the veins was argentiferous. Native silver from the leached zone of the C.O.D. mine is invariably associated with this ga-

lena and with secondary chalcocite, implying the native silver is a product of galena dissolution rather than a primary phase. Copper is the only commodity that was enriched during stage 4, by minor additions of chalcocite and covellite.

Wall-rock alteration: Owing to a lack of fresh exposures, wall-rock alteration associated with polymetallic quartz veins was not examined as part of this study. Thomas (1949) described alteration patterns on the 1,000-ft level of the Tennessee mine that show an evolution from (in our nomenclature) strong silicification within the vein structure, to intense quartz + sericite + pyrite alteration within 0.7 m of the vein, yielding to a similar but less strongly developed assemblage farther away; there is a strong argillic overprint immediately adjacent to the vein. Thomas (1949) observed similar alteration effects in hosts of differing rock type.

Metal zoning pattern: Eidel et al. (1968) and Wilkinson et al. (1982) presented metal zoning maps of the Wallapai district. The maps were based on mine production records, dump samples, and drill hole data, and the zones were drawn so as to be symmetrical around Mineral Park, and to extend into the west-central part of the district where very few data exist on which to base a zoning pattern. In Figure 4, we have maintained the boundaries of Wilkinson et al. (1982) throughout most of the district but have removed their zoning from the west-central region. Our zones are drawn for exposed deposits only, yielding a modified geometry that will be discussed in more detail below. The metal zones proceed outward from Mineral Park as follows: (1) Cu-Mo, (2) Cu and Mn, (3) Pb-Zn and As, and (4) Ag-Au (Fig. 4). The Mn and As enrichments in zones 2 and 3 were identified during this study. Similar zoning patterns are present at Bingham Canyon (John, 1978) and at Butte (Meyer et al., 1968).

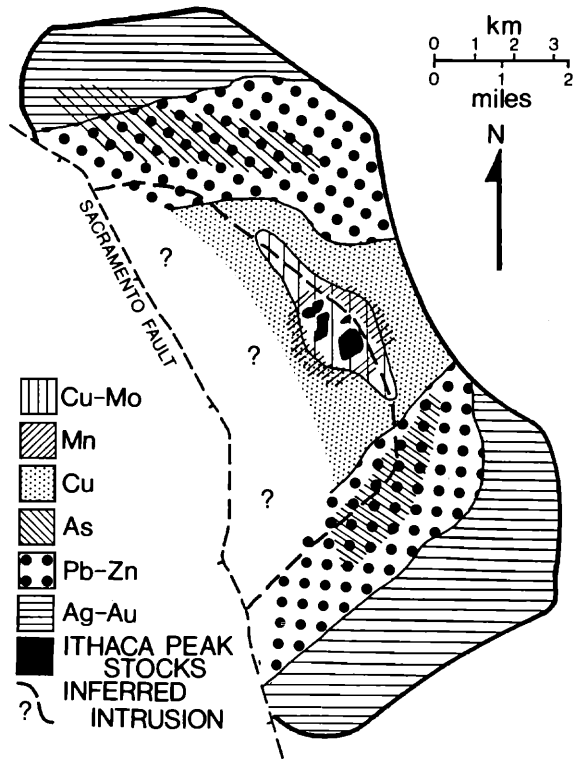

FIG. 4. Metal zoning patterns in the Wallapai mining district, modified from Eidel et al. (1968) and Wilkinson et al. (1982). The extrapolation of zoning patterns into the west-central portion of the district (unpatterned region) has been removed, and zones of high manganese and arsenic have been added.

Fluid Inclusion Petrography

Fluid inclusions were studied by standard heating and freezing techniques on an SGE gas-flow heating and freezing stage at the University of Arizona. The stage was calibrated with respect to the melting points of pure salts.

Fluid inclusions are abundant in all samples. After careful petrographic examination, fluid inclusions in quartz from each of the alteration and mineralization stages at Mineral Park, and from polymetallic quartz veins throughout the district, were studied. The observations and results reported here were obtained from extensive petrographic observations, 580 heating measurements, and 79 freezing measurements.

Fluid inclusions were classified by the phase relationships observed at room temperature, using the criteria of Nash (1976). Type I inclusions are of moderate salinity. They contain a water-rich liquid phase and a vapor bubble that occupies less than one-half of the cavity. They may contain daughter minerals other than halite. Type II inclusions are vapor dominated and are of low salinity. Type III inclusions are defined by the presence of a halite daughter mineral and may be either liquid or vapor rich. Fluid inclusions that contain a visibly separate CO_2-rich phase are classified as type IV.

Polymetallic quartz veins

Type I inclusions were the only type observed in vein quartz. No trapped or daughter minerals were observed. Primary inclusions were distinguished by their presence along growth planes in quartz. All primary inclusions are less than 8 μ in longest dimension, but secondary inclusions, occurring along fracture planes, range up to 20 μ. Shapes vary from negative crystal forms to amoeboid. No variation in the ratio of phase volumes was observed.

Quartz-pyrite veins

These veins contain secondary, fracture-controlled, type I inclusions; a second population of

type I inclusions found along quartz growth planes may be primary. No daughter minerals were observed and the ratio of vapor to liquid appears constant within any given group of inclusions. Sizes range up to 25 μ, with irregular shapes and negative crystal forms most common.

Anhydrite-molybdenite, quartz-molybdenite, and anhydrite-chalcopyrite veins

Fluid inclusions of types I, II, and III were observed in anhydrite-molybdenite and anhydrite-chalcopyrite veins, but only types I and II were found in the quartz-molybdenite veins. A single type IV fluid inclusion was observed. Gas chromatograph analyses of inclusion fluids at Mineral Park by Drake (1972) typically found between 0 and 3 mole percent CO_2 in type IA inclusions (see below). Crushing tests by the present authors did not reveal the presence of CO_2 in other inclusion types. We recognize the importance of even small amounts of carbon dioxide in the interpretation of fluid inclusion data in general, but the minor amounts of CO_2 suggested by the above data and by our observations will not affect the determination of salinity significantly in the context of this study. Neither will they inhibit the discrimination of inclusion populations of greatly different salinity—observations that are critically important here. Type IV inclusions will not receive further treatment.

Type I inclusions: Type I inclusions predominate in every sample, and three subtypes were noted during petrographic examination. Primary type I inclusions are rare, and in most cases, difficult to identify. Inclusions which occur isolated in the quartz host, and which do not have a geometric relationship with fractures or other nearby inclusions, may be primary and are called type IA inclusions. Type IA inclusions sometimes occur within recrystallized quartz. Type IB inclusions are a subtype that is spatially associated with type II inclusions. Types IB and II are found adhering to solid inclusions of anhydrite and biotite in both anhydrite-molybdenite and quartz-molybdenite veins, and very rarely in anhydrite-chalcopyrite veins. The third subtype, type IS, comprises inclusions contained within throughgoing fractures in quartz crystals; they are of secondary habit.

Sizes of all three subtypes range up to greater than 40 μ, with inclusions larger than 20 μ uncommon. Shapes are variable. Type IS inclusions tend toward small negative crystal forms, whereas type IA inclusions are larger and more irregular. Opaque minerals, probably pyrite and chalcopyrite, are commonly present in both type IA and type IS inclusions, but neither is found in type IB inclusions. The pyrite and chalcopyrite crystals vary in size relative to the volumes of the fluid inclusion cavities. The ratio of liquid to vapor appears constant in given groups of inclusions.

Type II inclusions: Vapor-rich fluid inclusions are much less abundant than type I or type III inclusions. Type II inclusions are usually found adhering to solid inclusions of anhydrite and biotite in the quartz-molybdenite veins; They are spatially associated with these same phases in the marginal quartz + molybdenite zones of the anhydrite-molybdenite veins. Adherence to solid inclusions is strongly suggestive of a primary habit (cf. Roedder, 1984). All type II inclusions are less than 10 μ long and have irregular shapes. No daughter minerals were observed.

Type III inclusions: Type III inclusions, like chalcopyrite, are concentrated in the central portions of the anhydrite-molybdenite and anhydrite-chalcopyrite veins and are most commonly found where chalcopyrite is abundant. Type III inclusions are randomly distributed in the host quartz, and some are attached to solid inclusions of chalcopyrite, suggesting that type III inclusions may represent the fluid that deposited chalcopyrite. The similarity of the daughter mineral assemblage in type III inclusions to the mineralogy of the anhydrite-chalcopyrite veins further suggests that this may be the case. Sizes range from 5 to 50 μ, with less than 18 μ most common. Shapes are amoeboid, and phase ratios appear constant between the fluid phase and most of the solids.

All type III inclusions contain halite as a daughter mineral. At Mineral Park, nine different included mineral phases have been observed, though no more than six occur in any single inclusion. The crystallographic and optical characteristics of the daughter minerals are consistent with the properties of halite, sylvite, calcite, anhydrite, chalcopyrite, pyrite, molybdenite, biotite, and possibly, sphalerite. All included minerals, with the exception of biotite and sphalerite, appear to have constant volume ratios with respect to the liquid and vapor phases, which suggests that they may be true daughter minerals. Because of their variable volume ratio to other phases, biotite and sphalerite are thought to be trapped phases.

Daughter minerals exhibit a crude zonation with depth in the deposit. Molybdenite occurs as a daughter mineral only in the deep samples 807-1301 and 807-1444, whereas chalcopyrite daughters were recognized only in 494-978 and samples above it. Sphalerite and calcite were noted only in the upper parts of the deposit, and acicular anhydrite daughters, though found at all levels in the system, are more common with increasing depth. The distribution of included minerals corresponds closely to the abundance of each mineral in the veins.

Fluid Inclusion Results

Polymetallic quartz veins

Sample locations (Fig. 5) span the length of the district and were selected to obtain information on each of the paragenetic stages described above. The data, from 16 samples, include 345 measurements from heating runs and 10 from freezing runs.

Type I inclusions homogenized to the liquid phase. Measurements were made on probable primary fluid inclusions, located along quartz growth planes or attached to solid inclusions, in every sample except those from the Golconda vein, where secondary and pseudosecondary fluid inclusions were used. The pressure-corrected results are shown in Figures 5 and 6. Pressure corrections (see below) add 30° to 40°C to the raw homogenization temperature data. In general, temperatures decrease outward from Mineral Park, from 410° to 420°C at the Jamison mine, 400° to 450°C at the Towne mine, and 420° to 440°C in sample 807-69 (drill core at Mineral Park) to 260° to 290°C at the Arizona Magma mine on the northern edge of the district and 290° to 320°C at the Champion mine on the southern periphery. Quartz from the Jamison mine hosts fluid inclusions along growth planes from paragenetic stages 1, 2a, and 3 that record a temperature decrease from 410° to 420°C (stage 1) to 300° to 340°C (stage 2a) to 160° to 180°C (stage 3) (Fig. 6). A temperature decrease was also observed at the C.O.D. mine, with stage 1 forming at 340° to 360°C, stage 2 at 230° to 280°C, and stage 3 at 160° to 180°C (Fig. 6).

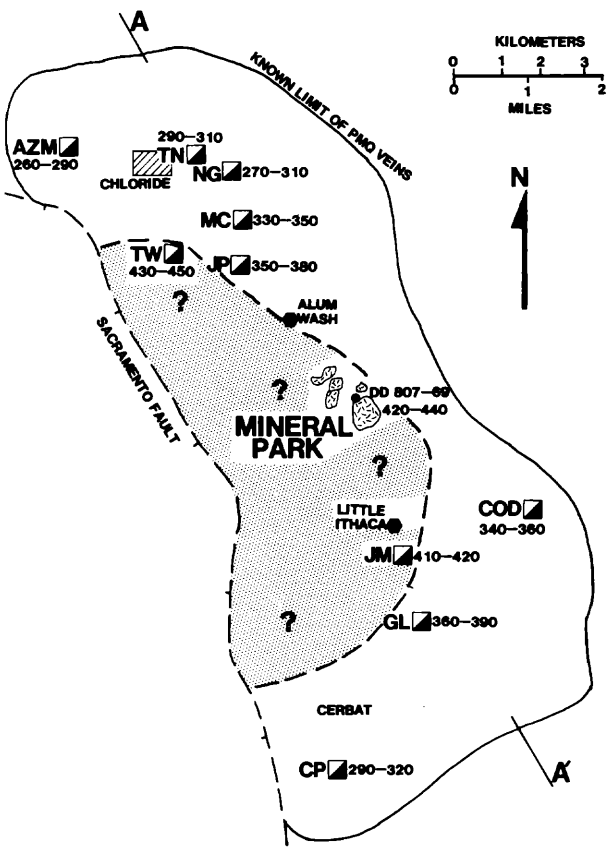

FIG. 5. Temperature zoning in polymetallic quartz (PMQ) veins. The ranges shown for each location are pressure-corrected homogenization temperatures of primary type I fluid inclusions from stage 1 mineralization (Fig. 6). The queried stippled pattern shows the limits of a suggested pluton beneath the polymetallic quartz veins with stage 1 temperatures greater than 400°C. Mine names are abbreviated: AZM-Arizona Magma, COD-C.O.D., CP-Champion, GL-Golconda, JM-Jamison, JP-Jupiter, MC-Minnesota-Conner, NG-North Georgia, TN-Tennessee, TW-Towne.

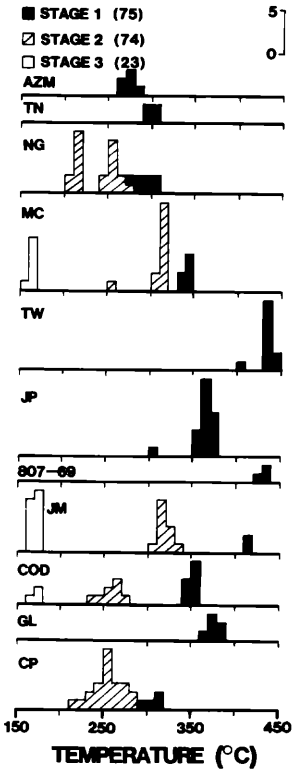

FIG. 6. Pressure-corrected homogenization temperatures of primary type I fluid inclusions in polymetallic quartz (PMQ) veins. The data are separated by stage of mineralization. The histograms are arranged in a general order of northwest at the top to southeast at the bottom, by projection onto the line A-A' of Figure 5. Number of data points in parentheses. Mine abbreviations as in Figure 5.

Salinities were determined using the freezing point depression equations of Potter et al. (1977b). All results fall within the range 1 to 7 equiv wt percent NaCl with no observable salinity difference between primary and secondary inclusions (Fig. 7A). No spatial or temporal changes in salinity were observed in this small data set.

Eutectic melting temperatures were recorded

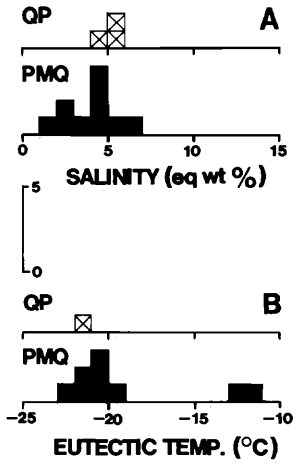

FIG. 7. Salinity (A) and eutectic melting temperature (B) of fluid inclusions in quartz-pyrite (QP) and polymetallic quartz (PMQ) veins. Data are from primary type I fluid inclusions along growth planes in quartz. Each stage of mineralization in the polymetallic quartz veins is represented.

from the few large primary inclusions available. The results cluster between −20° and −23°C (Fig. 7B), near the eutectic temperature of the H_2O-NaCl or H_2O-NaCl-KCl systems. Two measurements are near −11°C, the eutectic temperature of the H_2O-KCl system.

Quartz-pyrite veins

Six primary(?) type I inclusions from two quartz-pyrite veins were examined. The homogenization temperature range of these inclusions is 320° to 350°C (Fig. 8). Three salinity measurements give a narrow range of 4 to 6 equiv wt percent NaCl (Fig. 7A). Wilkinson (1981) noted a salinity range in these veins from 1 to 13 equiv wt percent NaCl. One eutectic temperature of −21.6°C was obtained (Fig. 7B), suggesting a simple H_2O-NaCl ± KCl chemistry.

Anhydrite-molybdenite, quartz-molybdenite, and anhydrite-chalcopyrite veins

Twelve samples from diamond drill core at Mineral Park were selected for study, with a vertical sample distribution of over 1,200 m (Fig. 2). References to these samples include a three digit drill hole identification number followed by depth from the collar in meters. The results were obtained by heating 285 inclusions of types IA, IB, II, and III and freezing 67 inclusions.

Type IA inclusions: Results of 218 heating runs on type IA fluid inclusions from these three vein types are shown in Figure 9. Type IA inclusions homogenize to the liquid phase. Uncorrected homogenization temperatures define broad peaks of 340° to 380°C in quartz-molybdenite veins and 310° to 370°C in the anhydrite-molybdenite and anhydrite-chalcopyrite vein stages. Specimens of individual anhydrite-molybdenite and anhydrite-chalcopyrite veins have narrower temperature ranges (Fig. 10).

The salinities of type IS and type IA inclusions were determined from the temperature of disappearance of ice ($T_{m_{ice}}$) and the freezing point depression equations of Potter et al. (1977b). Twelve type IS and 29 type IA inclusions were examined. The results are shown in Figure 8B. The salinities of type IA and type IS inclusions overlap and fall within the range of 1 to 17 equiv wt percent NaCl. Figure 8A shows 68 salinity determinations on type I inclusions from Wilkinson et al. (1982). Their petrographic descriptions do not allow us to separate type IA from IS, and some data for quartz-pyrite veins are also included. These uncertainties notwithstanding, the range of their data, 1 to 13 equiv wt percent NaCl, is nearly identical to the range for this study.

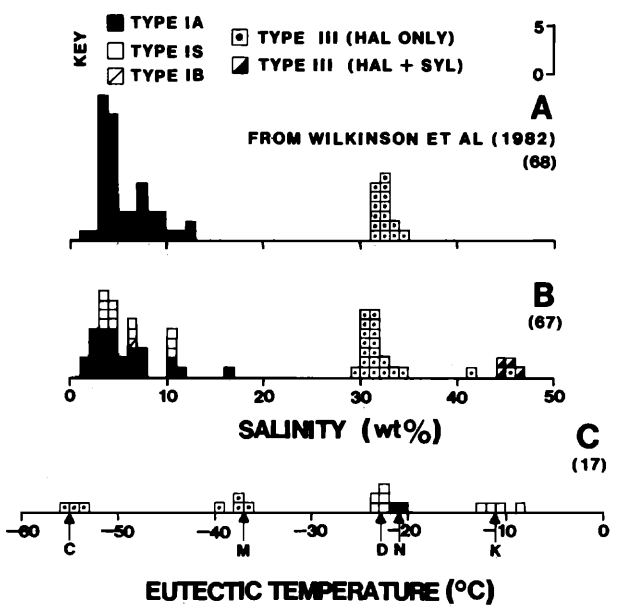

FIG. 8. Salinities and eutectic temperatures of fluid inclusions in anhydrite-molybdenite (AM) and anhydrite-chalcopyrite (AC) veins. A. Salinity data from Wilkinson et al. (1982). Inclusion types IA and IS are combined as IA, and some data from quartz-pyrite (QP) veins are also included. Type III inclusions are from a coarse-grained quartz + biotite vein that may be paragenetically earlier than the anhydrite-molybdenite veins. B. Salinities of various types of fluid inclusions from this study. Type III inclusions are separated on the basis of daughter salts. C. Eutectic temperature data from inclusion types IA, IS, and III, with all data for halite-, sylvite-, and halite + sylvite-bearing type III inclusions combined. Arrowed letters on the x-axis indicate the positions of eutectic temperatures of common aqueous chloride systems: C-NaCl-$MgCl_2$-$CaCl_2$, D-NaCl-KCl, K-KCl, M-NaCl-$MgCl_2$, N-NaCl. Number of data in parentheses.

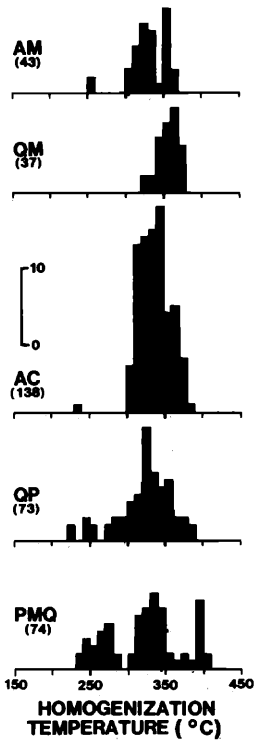

FIG. 9. Homogenization temperature data of type IA fluid inclusions from anhydrite-molybdenite (AM), quartz-molybdenite (QM), anhydrite-chalcopyrite (AC), and quartz-pyrite (QP) veins, compared with data for primary type I inclusions from stage 1 of the polymetallic quartz vein mineralization. The histogram for the quartz-pyrite veins combines data of this study with data from Wilkinson et al. (1982). Number of data in parentheses.

Two type IA inclusions from the anhydrite-molybdenite and anhydrite-chalcopyrite veins have eutectic temperatures near −23°C (Fig. 8C), corresponding to the ternary H_2O-NaCl-KCl system. Eutectic temperatures of type IS inclusions have a bimodal distribution with peaks near −22° and −11°C, similar to that noted above for primary type I inclusions in polymetallic quartz veins.

Type IB inclusions: Because of the rarity and small size of type IB inclusions, only 19 measurements were obtained. Figure 11 shows that most of the results are within the range 360° to 410°C in each of the anhydrite-molybdenite, quartz-molybdenite, and anhydrite-chalcopyrite veins. One salinity determination gave 6.8 equiv wt percent NaCl (Fig. 8B).

Type II inclusions: Type II inclusions homogenize to the vapor phase. Heating runs on type II inclusions (Fig. 11) show a temperature range of 360° to 420°C in the anhydrite-molybdenite, quartz-molybdenite, and anhydrite-chalcopyrite veins. Although the data are few, the overlap in the ranges of homogenization temperatures of type II inclusions and coexisting type IB inclusions is strongly suggestive of the coexistence of vapor and liquid in the system. The small size of these inclusions made observations of melting temperatures unreliable, but their coexistence with low-salinity type IB inclusions suggests that they also contain dilute brine.

Type III inclusions: The homogenization temperatures of type III inclusions from anhydrite-chalcopyrite veins, and the interior parts of anhydrite-molybdenite veins, are shown in Figures 10 and 11; no pressure correction has been applied. Type III inclusions homogenize to the liquid phase by the sequential disappearance of sylvite, halite, and lastly, the vapor phase. No change in size or optical characteristics of other included minerals was observed. Homogenization temperatures range from 200° to 380°C, with no apparent peak. The maximum range is 140°C for any individual sample (sample 807-1301; Fig. 10). The homogenization temperatures of type III inclusions invariably fall at or below the temperatures of type IB and II inclusions from the same sample (Fig. 10).

It should be noted that Wilkinson et al. (1982)

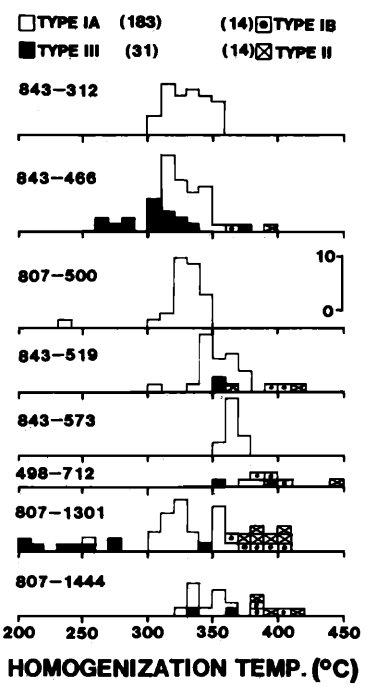

FIG. 10. Homogenization temperatures of fluid inclusion types IA, III, IB, and II from anhydrite-molybdenite (AM) and anhydrite-chalcopyrite (AC) veins, by individual sample. Samples are arranged in order of increasing depth from the surface (Fig. 2). Samples 807-1301, 807-1444, and the outer portion of 843-466 are anhydrite-molybdenite veins. All other samples are anhydrite-chalcopyrite veins. Type III inclusions in sample 843-466 are texturally related to an anhydrite-chalcopyrite mineral assemblage that has filled a reopened anhydrite-molybdenite vein. Number of data in parentheses.

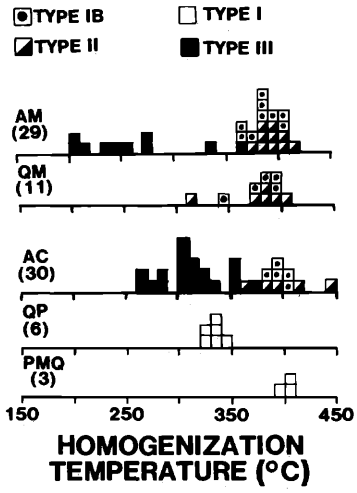

FIG. 11. Homogenization temperatures of inclusion types IB, II, and III from anhydrite-molybdenite (AM), quartz-molybdenite (QM), and anhydrite-chalcopyrite (AC) veins, compared with data from type I inclusions from quartz-pyrite (QP) and polymetallic quartz (PMQ) veins within the porphyry deposit. Data for the quartz-pyrite veins are from primary type I inclusions located along growth planes in vein quartz. Data for the polymetallic quartz veins come only from primary type I inclusions in stage 1 mineralization of sample 807-69. Number of data in parentheses.

reported the presence of type III fluid inclusions in a large, coarse-grained quartz + biotite vein, which is mineralogically similar to fine-grained quartz + biotite veinlets that are known to be paragenetically earlier than any of the sulfide-bearing vein stages (Table 1). They found a range in homogenization temperatures from 300° to 350°C, and a salinity range of 31 to 35 wt percent NaCl from the dissolution temperature of halite. Quartz + biotite veins were not examined in the current investigation, and the significance of these salt-rich fluids is uncertain.

Salinity and compositional data were obtained from freezing measurements on 26 inclusions. The salinity of inclusions containing a halite daughter mineral was obtained from the solution temperature of halite ($T_{m_{halite}}$) and the solubility data of Potter et al. (1977a). For inclusions containing both halite and sylvite daughter minerals, salinity was evaluated by applying the temperatures of solution of each salt to the ternary diagram of the NaCl-KCl-H_2O system presented by Roedder (1984). The ternary method may yield inaccurate results if additional aqueous components are present, as is very likely here, but it has been shown to give results roughly similar to leachate analyses of compositionally complex fluids (Eastoe, 1978).

The solution temperatures of sylvite (100°–124°C) and halite (245°–385°C) from type III inclusions containing both salts as daughter minerals gave 19 to 21 equiv wt percent NaCl (6.2 *m*) and 25 to 27 equiv wt percent KCl (6.1 *m*) (Fig. 8B). The *m*K/*m*Na ratio of 0.98 is higher than most published ratios from other porphyry deposits, such as 0.20 to 0.39 at Panguna (Eastoe, 1978) and 0.14 at Sierrita (Turner, 1983), but falls well within the 0.52 to 1.76 range of K/Na atomic ratios at Red Mountain (Bodnar and Beane, 1980). The salinities of type III inclusions containing halite without sylvite lie in the range 29 to 46 equiv wt percent NaCl (Fig. 8B). These latter results must be considered incomplete, however, as salinity can only be estimated in terms of the system NaCl-H_2O, whereas the solution may still contain appreciable, but unknown, quantities of KCl. Even though an inclusion may be saturated in KCl, nucleation problems might prevent sylvite precipitation (Eastoe, 1978). Salinity results for these fluids represent a minimum estimate only and cannot be compared directly to the more complete salinity determinations on inclusions containing both halite and sylvite. An additional uncertainty arises when divalent and trivalent chloride species are present, as is suggested by the eutectic temperature data below. These species may significantly affect the determinations of NaCl and KCl contents, although quantitative evaluations cannot yet be made (Crawford, 1981; Roedder, 1984).

The presence of halite and sylvite daughter minerals in type III inclusions suggests that NaCl and KCl were the dominant aqueous components in these fluids. Eutectic temperature measurements of −55° to −57°C and −35° to −39°C on some inclusions (Fig. 8C) require the presence of additional aqueous components. Roedder (1984) stated that the only geologically reasonable component that can lower eutectic temperatures below −50°C is $CaCl_2$, but he also gave a value of −55°C for the H_2O-$FeCl_3$ system. Iron chlorides are known to be important in other ore systems, such as Panguna (Eastoe, 1978), so this component should not be excluded. Eutectic temperatures near −37°C suggest that a magnesium component may be present. The fluids responsible for chalcopyrite mineralization in anhydrite-molybdenite and anhydrite-chalcopyrite veins can probably best be described in terms of the complex system H_2O-NaCl-KCl-$CaCl_2$-$MgCl_2$-$FeCl_2$ (or $FeCl_3$), on which no data exist.

Relationship of anhydrite-molybdenite, quartz-molybdenite, and anhydrite-chalcopyrite veins

The textural and mineralogical variations between edges and centers of anhydrite-molybdenite veins also correlate with changes in fluid inclusion populations, from types IB and II at the vein margin, to type III at the center. The mineral assemblage and fluid inclusion population of the quartz-molybdenite veins is almost identical to the marginal as-

semblage of the anhydrite-molybdenite veins. Anhydrite-chalcopyrite veins, on the other hand, differ from quartz-molybdenite veins and the outer parts of anhydrite-molybdenite veins in their texture, mineralogy, and fluid inclusion populations but are similar to the interior portions of anhydrite-molybdenite veins. In one case (sample 843-446), textures suggest that an anhydrite-chalcopyrite assemblage may have filled the center of a reopened quartz-molybdenite or anhydrite-molybdenite vein. Thus, although quartz-molybdenite and anhydrite-chalcopyrite veins appear to be distinct, the relationship of anhydrite-molybdenite veins to both is less clear. Anhydrite-molybdenite veins may result from either (1) an anhydrite-chalcopyrite filling of reopened quartz-molybdenite veins, in which case the reported paragenetic relationship between anhydrite-molybdenite and quartz-molybdenite veins is not generally valid, or (2) a change in fluid physicochemical characteristics within the time span of formation of the anhydrite-molybdenite vein set itself, with early boiling fluids being succeeded by salt-rich liquid. The latter scenario is less plausible, as no inclusions with salinities intermediate between those of the dilute inclusions of types IB and II and the hypersaline inclusions of type III have been observed. Inclusions of intermediate salinity would be expected if a gradational fluid change had actually occurred. Type III inclusions in the center of anhydrite-molybdenite sample 807-1301, for example, could be explained by reopening and filling of the vein, though textural evidence for this is lacking, or they could be of secondary origin, introduced during formation of later stage anhydrite-chalcopyrite veins. These uncertainties notwithstanding, the consistent spatial separation of molybdenite and chalcopyrite into zones of differing textural characteristics and coexisting mineral assemblages implies that different depositional conditions prevailed during molybdenite and chalcopyrite introduction.

Type IA inclusions in anhydrite-molybdenite, quartz-molybdenite, anhydrite-chalcopyrite, and quartz-pyrite veins

Annealing textures, such as 120° intersections of grain boundaries, were observed in some groups of quartz grains in the anhydrite-molybdenite and anhydrite-chalcopyrite veins. Although we cannot be certain of the identity of the fluids responsible for this recrystallization, they may be represented among the type IA fluid inclusions that predominate in the anhydrite-molybdenite, quartz-molybdenite, anhydrite-chalcopyrite, and quartz-pyrite veins at Mineral Park. If this is the case, type IA inclusions may be the primary inclusions in newly crystallized quartz but would be secondary in earlier grains. This could account for the ambiguity in habit of type IA inclusions, noted above, as well as their similarity to type IS inclusions. Assuming that this scenario is plausible, most of the primary fluid inclusions of types IB, II, and III that represent the formative fluids of the early vein stages may have been removed during an episode of hydrothermal "reworking" of vein quartz—this also accounting for their paucity. Type IA inclusions resemble the primary type I inclusions found along quartz growth planes in the polymetallic quartz veins in petrographic characteristics, fluid chemistry (Drake, 1972), and the peak temperatures observed in each vein stage (Fig. 9). An exception to this is that type IA inclusions commonly contain opaques, probably pyrite, and chalcopyrite, as included minerals. These opaques could have been derived from reopened type III fluid inclusions during the later hydrothermal event that affected quartz.

Pressure and Depth

The diagrams of Sourirajan and Kennedy (1962) indicate a trapping pressure of 250 to 300 bars for the coexisting type IB and II inclusions in anhydrite-molybdenite, quartz-molydenite, and anhydrite-chalcopyrite veins. The inclusions homogenize at approximately 400°C and have average salinities of about 5 equiv wt percent NaCl.

Homogenization temperatures of type III inclusions from the central zones of veins are up to 150°C lower than type II and IB inclusions from the margin of the same vein (Fig. 10). Bodnar and Beane (1980) observed a similar phenomenon at Red Mountain, Arizona, where early boiling fluids at 400°C and 250 bars were succeeded by type III inclusions with homogenization temperatures as much as 100°C lower. Because fluids trapped at a constant temperature will yield progressively lower homogenization temperatures as pressure increases, Bodnar and Beane (1980) attributed the 100°C temperature decrease to a change in pressure regime from 250 bars hydrostatic pressure to 1,000 bars lithostatic pressure, as veins became sealed by mineral deposition. The situation of Mineral Park may be analogous and a similar interpretation is adopted here. In sample 843-466, homogenization temperature of type III fluid inclusions from the center of the vein range from values equivalent to those of type IB and II inclusions on the edge of the vein to temperatures 100°C lower (Fig. 10). The pressure correction curves of Potter (1977) indicate that an increase in pressure of about 800 bars could account for the homogenization temperature decrease. If this is what happened at Mineral Park, pressure is interpreted to have increased from 300 bars hydrostatic pressure (corre-

sponding to 3 km deep) to about 1,100 bars lithostatic pressure (corresponding to 4 km burial).

Drake (1972) performed gas chromatograph analyses on inclusion fluids from the five sulfide-bearing vein stages to determine their H_2O, CO_2, CH_4, and H_2 concentrations. The results of Drake (1972) provide mole percent CO_2, temperature, and salinity data on individual fluid inclusions which may be applied to the CO_2 solubility curves of Takenouchi and Kennedy (1964, 1965), as modified by Roedder and Bodnar (1980), to obtain a minimum fluid trapping pressure, although this method is of uncertain accuracy. Petrographic descriptions, homogenization temperatures, and salinity results show that the fluid inclusions examined by Drake (1972) correspond to the type IA inclusions of this study. The samples Drake (1972) obtained were from the pit and shallow drill holes, and the average minimum trapping pressure near the pit level is approximately 350 bars. Using an average salinity of 10 equiv wt percent NaCl, the curves of Potter (1977) give pressure-corrections of 35° to 54°C for type IA inclusions and 30° to 40°C for type I inclusions in polymetallic quartz veins.

To summarize, the 250- to 300-bars pressure during liquid-vapor coexistence gives a depth range of 2.5 to 3 km (hydrostatic regime) to about 1 km (lithostatic regime). A depth of burial of 3 to 4 km is suggested by the pressure increase scenario for type III inclusions. During the formation of type IA inclusions, a pressure of 350 bars, from the data of Drake (1972), corresponds to a burial depth of 3.5 km for a purely hydrostatic pressure regime (100 bars/km) or 1.3 km for a purely lithostatic (270 bars/km) regime. Wilkinson (1981) estimated a burial depth of about 3 km from restored stratigraphy. The similarity among estimates of formation depth by these varied approaches suggests that 3 to 4 km may be considered a reasonable depth of mineralization.

Discussion

Hydrothermal evolution at Mineral Park

Fluid inclusion data now available indicate a succession of five distinctive hydrothermal regimes during the formation of the Mineral Park deposit. In order, these are: (1) a salt-rich liquid that deposited quartz + biotite (Wilkinson et al., 1982), (2) boiling, low-salinity brines that deposited molybdenite-bearing assemblages, (3) salt-rich liquid that apparently deposited chalcopyrite-bearing assemblages, (4) low-salinity, nonboiling brines that deposited quartz-pyrite veins, and (5) low-salinity, nonboiling brines of higher temperature than for (4), depositing polymetallic quartz veins. Alteration assemblages containing biotite and K-feldspar are associated with the first three regimes, and assemblages containing sericite, chlorite, and calcite are associated with the last two. As suggested by the conflicting indications on the relationships of anhydrite-molybdenite and quartz-molybdenite veins, there may be additional complexities, but these are of second order within the framework outlined.

Origins of hydrothermal fluids

The very high salinity of the type III inclusions in the anhydrite-chalcopyrite and anhydrite-molybdenite veins suggests that these fluids are predominantly of magmatic derivation. The Permian Kaibab Formation and the Jurassic Carmel Formation may have been part of the overburden to these deposits, however, and a salinity contribution from dissolution of evaporites in these units cannot be wholly discounted. A magmatic derivation of these fluids is consistent with the theoretical predictions of Candela and Holland (1986), who showed that copper in porphyry systems may be derived from crystallizing magmas and transported in chloride-rich fluids, and with the observations of Eastoe and Eadington (1986), who described apparently primary inclusions of very high salinity in quartz phenocrysts at the Panguna deposit. The low salinities and apparently simple aqueous chemistry of the fluids contained in the primary type I inclusions in the quartz-pyrite and polymetallic quartz veins are consistent with a predominantly meteoric origin. The boiling, low-salinity fluids that introduced molybdenite could be of either magmatic or meteoric origin, or a mixture of the two; the fluid inclusion evidence is not sufficient to discriminate between these possibilities. Candela and Holland (1986), however, demonstrated that molybdenum may be efficiently extracted from magmatic bodies by low-salinity magmatic fluids.

These conclusions are consistent with stable isotope studies of the porphyry environment. Oxygen and hydrogen isotope studies, summarized by Taylor (1979), suggest that quartz + sericite + pyrite alteration assemblages in porphyry orebodies (equivalent to the quartz-pyrite veins at Mineral Park) are generally formed by late-stage hydrothermal fluids composed predominantly of meteoric water. Biotites associated with potassic alteration (represented here by anhydrite-molybdenite, quartz-molybdenite, and anhydrite-chalcopyrite veins) in other porphyry systems, e.g., Butte, Santa Rita, Bingham, and Ely, are derived from waters of consistent isotopic composition, probably magmatic fluids.

Relationship of the porphyry-style mineralization to Laramide intrusions

In the lithocap region above a cooling pluton, NaCl solutions attain temperatures of 300° to

400°C for extended periods of time (Norton, 1979). This is the temperature range indicated by primary fluid inclusions at Mineral Park, which have peaks of about 400°C for anhydrite-molybdenite, quartz-molybdenite, and anhydrite-chalcopyrite veins, and 320° to 350°C for quartz-pyrite veins. Wilkinson (1981) notes a lack of high-temperature (greater than 500°C) fluid inclusions. These high-temperature fluids are characteristic of the immediate pluton environment and typically accompany mineralization that is close to the causative pluton, for example, at Santa Rita, New Mexico (Reynolds and Beane, 1985), and at Panguna (Eastoe, 1978). The absence of high-temperature fluids suggests that the porphyry mineralization is not directly related to the exposed Ithaca Peak stocks (Wilkinson et al., 1982). A hydrothermal system with fluid inclusion populations, vein mineralogy, alteration, and fluid compositions similar to those at Mineral Park existed at Red Mountain, Arizona, where the causative pluton is neither exposed nor encountered in the 1.5-km limit of deep drilling (Bodnar, 1978).

Fracture patterns, on the other hand, suggest that porphyry-style mineralization was approximately contemporaneous with the exposed Laramide stocks. Wilkinson (1981) found that the orientation of the early vein sets was controlled by stress patterns and thermal perturbations of pore fluids during emplacement of the Ithaca Peak stocks. This initial intrusive control yielded to the regional northeast-southwest stress pattern that prevailed during the main Laramide phase of porphyry mineralization in Arizona (Rehrig and Heidrick, 1972) during formation of the late-stage quartz-pyrite and polymetallic quartz veins.

The Alum Wash prospect and the Little Ithaca altered area are removed from the Ithaca Peak stocks by 2 and 4 km, respectively (Fig. 1), yet both contain potassium feldspar + biotite alteration and anomalous copper and molybdenum values (Vega, 1984). Importantly, no intrusion has been found in either area, either exposed or in deep drill holes. Also, there is no continuous alteration zone between these three areas.

The clear separation of these three distinct altered and mineralized areas, their occurrence at fold-intrusive contact intersections that may well have had an enhanced structural permeability, and the fracture control exerted by the Ithaca Peak stocks on the orientations of early-stage porphyry-style veins may all reflect the migration of mineralizing fluids along structurally favorable channelways, from a source lying at a deeper level than the exposed Laramide stocks. The emplacement of the Ithaca Peak stocks may have generated the greatest permeability in the three, explaining why the main mineralization is located at Mineral Park, rather than at Alum Wash or Little Ithaca.

Relationship of polymetallic quartz veins to porphyry-style mineralization

The Mineral Park deposit occurs at the geographic center of the Wallapai mining district. Homogenization temperatures of primary type I fluid inclusions from stage 1 mineralization in polymetallic quartz veins decrease away from Mineral Park toward the district periphery (Figs. 5 and 6). Temperatures decrease by 170°C to the north and by 120°C to the south, but the detail of the temperature zoning is not symmetrical about the Ithaca Peak stocks, suggesting a different heat source, or additional sources. The model studies of Norton (1979, 1982) indicate that intrusions the size of the Ithaca Peak stocks could not produce a 20-km-long district with 300°C peripheral temperatures. A much larger body would be required to supply the necessary heat. One possible orientation of this large inferred body is indicated in Figure 3; its limits were taken to lie beneath the polymetallic quartz veins with peak stage 1 temperatures of greater than 400°C. The temperatures in the remaining polymetallic quartz veins, all with peak values of less than 400°C, are as easily related to the inferred intrusion as to the Ithaca Peak stocks. Much the same symmetry is evident in the modified metal zonation map (Fig. 5). A considerable portion of the district may have been faulted away to the west by the basin-and-range Sacramento fault and may now lie buried beneath the alluvium of the Sacramento Valley, as suggested in Figures 3 and 4. Wilkinson et al. (1982) described a gravity low beneath the Wallapai mining district. The low coincides with the distribution of dikes and polymetallic quartz veins and was explained by the possible presence of a larger intrusive body beneath the district by these authors.

It was noted above that the exact age of the polymetallic quartz veins has not been established. They are known to be younger than the anhydrite-molybdenite, quartz-molybdenite, anhydrite-chalcopyrite, and quartz-pyrite veins in the porphyry-style deposit and younger than Laramide rhyolite dikes which are coeval with porphyry mineralization. Geologic relations do not allow for a minimum age limit to be placed. A mid-Tertiary age for these veins is possible, and they could be related to extensive mid-Tertiary volcanism in the district (Thomas, 1953).

Similar polymetallic veins, in many cases brecciated, are reported as the final stage of mineralization in many other porphyry-style deposits, e.g., Panguna (Eastoe, 1978), Chuquicamata (Alvarez

and Flores, 1986), Morenci (R. Preece, pers. commun., 1987), Hall (Shaver, 1986), Bell Copper (Carson et al., 1976), Island Copper (Cargill et al., 1976), Morrison (Carson and Jambor, 1976), Buckingham (Loucks and Johnson, 1983), Mount Emmons (Thomas and Galey, 1982), and Kitsault (Steininger, 1985). The presence of such veins within porphyry-style deposits is common and may be characteristic of this deposit class. It is therefore unlikely to represent a chance superposition of unrelated events at Mineral Park. Whether a late intrusive event is required to generate the polymetallic veins in all cases is unclear, although many of these districts do have a history of multiple intrusion. Very few temperature data exist for cases other than Mineral Park.

Relationship of quartz-pyrite veins to other stages of mineralization

The quartz-pyrite veins, with their sericitic selvedges (Wilkinson et al., 1982), are equivalent to the phyllic alteration zone found in most porphyry-style deposits (Titley, 1982a). At Mineral Park this phyllic zone does not involve an extensive volume of rock with respect to the Wallapai district as a whole. Fluid inclusion data indicate that the quartz-pyrite veins formed from low-salinity waters at temperatures 50° to 100°C lower than the paragenetically earlier anhydrite-molybdenite, quartz-molybdenite, and anhydrite-chalcopyrite veins (Fig. 11). The quartz-pyrite veins also formed at temperatures about 100°C lower than polymetallic quartz veins, which crosscut them in the porphyry deposit itself and were also deposited from low-salinity waters. The abrupt increase in temperature from quartz-pyrite to polymetallic quartz veins suggests that they formed from different hydrothermal systems. The fluids that deposited the quartz-pyrite veins probably represent the waning stages of heated meteoric waters convecting about the Mineral Park porphyry deposit, whereas fluids that deposited the polymetallic quartz veins, probably also of predominantly meteoric derivation, were mobilized by a later input of heat beneath a broad area of the district, perhaps because of a later pulse of magma at depth.

Conclusions

1. Molybdenite mineralization in the quartz-molybdenite veins formed from dilute boiling brines at 370° to 410°C.

2. Anhydrite-molybdenite veins are zoned, with edges identical both texturally and mineralogically to the quartz-molybdenite veins and centers that resemble the anhydrite-chalcopyrite veins. Molybdenite occurs only at the vein edges, in association with dilute boiling fluids at 360° to 410°C. Minor chalcopyrite was introduced in the central parts of these veins from nonboiling highly saline brines of more than 44 wt percent total salts, with temperatures of associated type III inclusions ranging up to a peak of 370°C.

3. The main introduction of copper occurred in the anhydrite-chalcopyrite veins from nonboiling high-salinity fluids that average 25 equiv wt percent KCl and 20 equiv wt percent NaCl at temperatures of 380° to 420°C. Additional aqueous components such as Mg, Ca, and Fe chlorides are indicated.

4. The quartz-pyrite veins formed from H_2O + NaCl fluids of 1 to 13 equiv wt percent NaCl, with homogenization temperatures of 320° to 350°C.

5. The polymetallic quartz veins formed in four distinct stages of mineralization, from fluids of 1 to 7 equiv wt percent NaCl. Only NaCl, and possibly KCl, was an important fluid constituent. Temperatures decreased with time from more than 400° C in stage I to less than 200°C in Stage III.

6. By analogy with other deposits, and consistent with the theoretical studies of Candela and Holland (1986), molybdenite and chalcopyrite probably were deposited by magmatic fluids. The later quartz-pyrite and polymetallic quartz veins are inferred to have originated from convecting meteoric fluids.

7. Both temperature and metal zoning patterns of the polymetallic quartz veins are asymmetrical about the exposed Ithaca Peak stocks but are consistent with fomation about a larger intrusion at depth.

8. The hydrothermal systems that formed the quartz-pyrite veins, and later formed the polymetallic quartz veins, were separate events. Quartz-pyrite veins formed from a small convection cell, localized near the Ithaca Peak stocks, at 320° to 350°C. Polymetallic quartz veins formed later from a much larger and hotter system which may have been related to an intrusion at depth.

9. Pressures may have increased from 250 to 300 bars during molybdenite mineralization, to approximately 1,100 bars during chalcopyrite mineralization, with a concomitant change from hydrostatic to lithostatic regimes. Indicated depths are 3 to 4 km, consistent with reconstructed stratigraphy.

10. The porphyry deposit is not directly related to the exposed Laramide intrusions but rather formed in a lithocap environment above a suggested larger intrusion at depth (Wilkinson et al., 1982), similar to the Red Mountain system (Bodnar and Beane, 1980). The geologic and fluid inclusion evidence suggests that the Ithaca Peak stocks were not directly related to mineralization in the district but

that fracturing associated with their emplacement served to facilitate the ascent of mineralizing fluids from depth.

11. The extensive zone of polymetallic quartz veins is not directly related to the main porphry mineralization but is probably related to a slightly younger, but broadly coeval, Laramide intrusion(s) centered beneath the Wallapai district (Fig. 12).

Acknowledgments

This study formed a portion of the Master's thesis research of the senior author. Special thanks are due John Guilbert, Austin Long, and Spencer Titley for reviewing and commenting on the work. Tom Connelly is also thanked for advice on locating useful information about the area. The Duval Corporation is gratefully acknowledged for the financial assistance it provided. Special thanks go to G. P. Boone, resident manager at the Mineral Park mine, and to Will Wilkinson and Luis Vega, then Duval Corporation geologists, for helpful discussions and logistical assistance. The cooperation of Allanco, Ltd., and George Parker are appreciated for underground access at the C.O.D. mine. The Department of Geosciences at the University of Arizona is also acknowledged for the provision of funds in support of field aspects of the study.

March 27, December 22, 1987

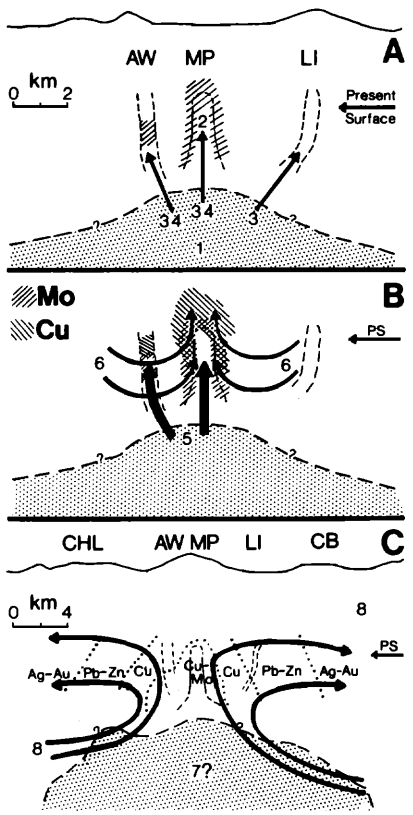

FIG. 12. Possible sequence of events during formation of the Wallapai mining district. Numbers denote the sequence: (1) emplacement of a large magmatic body at depth, (2) emplacement of the Ithaca Peak stocks as apophyses of this pluton, (3) upward-moving fluids form the selectively pervasive potassic alteration, (4) boiling fluids form the molybdenum orebody, (5) high-salinity fluids form the copper mineralization, (6) a convection cell composed of meteoric water forms the phyllic alteration zone, (7) additional intrusion at depth possible, (8) a large convection cell of predominately meteoric water forms polymetallic quartz veins, driven by heat from the large pluton(s) at depth. In C, copper and molybdenum mineralization patterns are omitted for clarity. The metal zones are as shown in Figure 4; the horizontal scale of C is twice that in A and B. AW = Alum Wash, CB = Cerbat, CHL = Chloride, LI = Little Ithaca, MP = Mineral Park.

REFERENCES

Alvarez, O., and Flores, R., 1986, Alteration and hypogene mineralization in the Chuquicamata porphyry copper deposit: Soc. Econ. Geologists Chile Field Trip Guidebook, Santiago, Chile, March, 1986, p. 151–173.

Bastin, E. S., 1925, Origin of certain rich silver ores near Chloride and Kingman, Arizona: U. S. Geol. Survey Bull. 750, p. 17–39.

Bodnar, R. J., 1978, Fluid inclusion study of the porphyry copper prospect at Red Mountain, Arizona: Unpub. M.S. thesis, Tucson, Univ. Arizona, 70 p.

Bodnar, R. J., and Beane, R. E., 1980, Temporal and spatial variations in hydrothermal fluid characteristics during vein filling in preore cover overlying deeply buried porphyry copper-type mineralization at Red Mountain, Arizona: ECON. GEOL., v. 75, p. 876–893.

Candela, P. A., and Holland, H. D., 1986, A mass transfer model for copper and molybdenum in magmatic hydrothermal systems: The origin of porphyry-type ore deposits: ECON. GEOL., v. 81, p. 1–19.

Cargill, D. G., Lamb, J., Young, M. J., and Rugg, E. S., 1976, Island copper: Canadian Inst. Mining Metallurgy Spec. Vol. 15. p. 264–273.

Carson, D. J. T., and Jambor, J. L., 1976, Morrison: Geology and evolution of a bisected annular porphyry copper deposit: Canadian Inst. Mining Metallurgy Spec. Vol. 15, p. 264–273.

Carson D. J. T., Jambor, J. L., Ogryzlo, P. L., and Richards, T. A., 1976, Bell copper: Geology, geochemistry and genesis of a supergene-enriched, biotitized porphyry copper deposit with a superimposed phyllic zone: Canadian Inst. Mining Metallurgy Spec. Vol. 15, p. 264–273.

Crawford, M. L., 1981, Phase equilibria in aqueous fluid inclusions: Mineralog. Assoc. Canada Short Course Handbook, v. 6, p. 75–100.

Dings, M. G., 1951, The Wallapai mining district, Cerbat Mountains, Mohave County, Arizona: U. S. Geol. Survey Bull. 978-E, p. 123–163.

Drake, W. E., 1972, A study of ore-forming fluids at the Mineral Park porphyry copper deposit, Kingman, Arizona: Unpub. Ph.D dissert. New York, Columbia Univ., 245 p.

Eastoe, C. J., 1978, A fluid inclusion study of the Panguna porphyry copper deposit, Bougainville, Papua New Guinea: ECON. GEOL., v. 73, p. 721–748.

Eastoe, C. J., and Eadington, P. J., 1986, High-temperature fluid inclusions and the role of the biotite granodiorite in mineralization at the Panguna porphyry copper deposit, Bougainville, Papua New Guinea: ECON. GEOL., v. 81, p. 478–483.

Eaton, L. G., 1980, Geology of the Chloride mining district, Mohave County, Arizona: Unpub. M.S. thesis, Soccoro, New Mexico Inst. Mining Technology, 133 p.

Eidel, J. J., Frost, J. E., and Clippinger, D. M., 1968, Copper-mo-

lybdenum mineralization at Mineral Park, Mohave County, Arizona, *in* Ridge, J. D., ed., Ore deposits of the United States, 1933–1967 (Graton-Sales vol.): New York, Am. Inst. Mining Metall. Petroleum Engineers, v. 2, p. 1258–1281.

Garrett, S. K. 1938, Tennessee-Schuylkill mine: Arizona Bur. Mines Bull. No. 145, Geology Ser. No. 12, p. 117–119.

John, E. C., 1978, Mineral zones in the Utah copper orebody: ECON. GEOL., v. 73, p. 1250–1259.

Loucks, T. A., and Johnson, C. A., 1983, Geology of the Buckingham molybdenum deposit, Lander County, Nevada [abs.]: Geol. Soc. America Abstracts with Programs, v. 15, p. 276.

Mauger, R. L., and Damon, P. E., 1965, K-Ar ages of Laramide magmatism and copper mineralization in the southwest: Atomic Energy Comm. Ann. Prog. Rept. COO-689-50, p. A-II-1–A-II-8.

Meyer, C., Shea, E. P., Goddard, C. C., Jr., and staff, 1968, Ore deposits at Butte, Montana, *in* Ridge, J. D., ed., Ore deposits of the United States, 1933–1967 (Graton-Sales vol.): New York, Am. Inst. Mining Metall. Petroleum Engineers, v. 2, p. 1373–1416.

Nash, J. T., 1976, Fluid inclusion petrology-data from porphyry copper deposits and applications to exploration: U. S. Geol Survey, Prof. Paper 907-D, 16 p.

Norton, D. L., 1979, Transport phenomena in hydrothermal systems: The redistribution of chemical components around cooling magmas: Bull. Mineralogie, v. 102, p. 471–486.

—— 1982, Fluid and heat transport phenomena typical of copper bearing pluton environments, southeastern Arizona, *in* Titley, S. R., ed., Advances in geology of the porphyry copper deposits, southwestern North America: Tucson, Univ. Arizona Press, p. 59–72.

Potter, R. W., II, 1977, Pressure corrections for fluid inclusion homogenization temperatures based on the volumetric properties of the system NaCl-H_2O: U. S. Geol. Survey Jour. Research, v. 5, p. 603–607.

Potter, R. W., II, Babcock, R. S., and Brown, D. L. 1977a, A new method for determining the solubility of salts in aqueous solutions at elevated temperatures: U. S. Geol Survey Jour. Research, v. 5, p. 389–395.

Potter, R. W., II, Clynne, M. A., and Brown, D. L., 1977b, Freezing point depression of aqueous sodium chloride solutions: ECON. GEOL., v. 73, p. 284–285.

Rehrig, W. A., and Heidrick, T. L., 1972, Regional fracturing in Laramide stocks of Arizona and its relationship to porphyry copper mineralization: ECON. GEOL., v. 67, p. 198–213.

Reynolds, T. J., and Beane, R. E., 1985, Evolution of hydrothermal fluid characteristics at the Santa Rita, New Mexico, porphyry copper deposit: ECON. GEOL., v. 80, p. 1328–1347.

Roedder, E., 1984, Fluid inclusions: Rev. Mineralogy, v. 12, 646 p.

Roedder, E., and Bodnar, R. J., 1980, Geologic pressure determinations from fluid inclusion studies: Ann. Rev. Earth Planet. Sci., v. 8, p. 263–301.

Shafiqullah, M., Damon, P. E., Lynch D. J., Reynolds, S. J., Rehrig, W. A., and Raymond, R. H., 1980, K-Ar geochronology and geologic history of southwestern Arizona and adjacent areas: Geol. Soc. Arizona Digest, v. 12, p. 201–260.

Shaver, S. A., 1986, Elemental dispersion associated with alteration and mineralization at the Hall (Nevada Moly) quartz monzonite-type porphyry molybdenum deposit, with a section on comparison of dispersion patterns with those from Climax-type deposits: Jour. Geochem. Explor., v. 25, p. 81–98.

Silver, L. T., 1967, Apparent age relations in the older Precambrian stratigraphy of Arizona [abs.]: Internat. Union Geol. Sci. Comm. Geochronology Conf. on Precambrian Stratified Rocks, Edmonton, Canada, August 1966, 87 p.

Sourirajan, S., and Kennedy, G. C., 1962, The system H_2O-NaCl at elevated temperatures and pressures: Am. Jour. Sci., v. 260, p. 115–141.

Steininger, R. C., 1985, Geology of the Kitsault molybdenum deposit, British Columbia: ECON. GEOL., v. 80, p. 57–71.

Takenouchi, S., and Kennedy, G. C., 1964, The binary system H_2O-CO_2 at high temperatures and pressures: Am. Jour. Sci., v. 262, p. 1055–1074.

—— 1965, The solubility of carbon dioxide in NaCl solutions at high temperatures and pressures: Am. Jour. Sci., v. 263, p. 445–454.

Taylor, H. P., Jr., 1979, Oxygen and hydrogen isotope relationships in hydrothermal mineral deposits, *in* Barnes, H. L., ed., Geochemistry of hydrothermal ore deposits: New York, Wiley Intersci., p. 236–277.

Thomas, B. E., 1949, Ore deposits of the Wallapai district, Arizona: ECON. GEOL., v. 44, p. 663–705.

—— 1953, Geology of the Chloride quadrangle Arizona: Geol. Soc. America Bull., v. 64, p. 391–420.

Thomas, J. A., and Galey, J. T., Jr., 1982, Exploration and geology of the Mt. Emmons molybdenite deposits, Gunnison County, Nevada: ECON. GEOL., v. 77, p. 1085–1104.

Titley, S. R., 1982a, The style and progress of mineralization and alteration in porphyry copper systems, American southwest, *in* Titley, S. R., ed., Advances in geology of the porphyry copper deposits, southwestern North America: Tucson, Univ. Arizona Press, p. 93–116.

—— 1982b, Some features of tectonic history and ore genesis in the Pima mining district, Pima County, Arizona, *in* Titley, S. R. ed., Advances in geology of the porphyry copper deposits, southwestern North America: Tucson, Univ. Arizona Press, p. 387–406.

Turner, K., Jr., 1983, The determination of the sulfur isotopic signature of an ore-forming fluid from the Sierrita porphyry copper deposit, Pima County, Arizona: Unpub. M.S. thesis, Tucson, Univ. Arizona, 93 p.

Vega, L. A., 1984, The alteration and mineralization of the Alum Wash prospect, Mohave County, Arizona: Unpub. M.S. thesis, Tucson, Univ. Arizona, 57 p.

Wilkinson, W. H., 1981, The distribution of alteration and mineralization assemblages of the Mineral Park mine, Mohave County, Arizona: Unpub. Ph.D. dissert., Tucson, Univ. Arizona, 101 p.

Wilkinson, W. H., Vega, L. A., and Titley, S. R., 1982, Geology and ore deposits at Mineral Park, Mohave County, Arizona, *in* Titley, S. R., ed., Advances in geology of the porphyry copper deposits, southwestern North America: Tucson, Univ. Arizona Press, p. 523–542.